

SPIN STRUCTURE OF THREE-NUCLEON BOUND STATES

V. Kotlyar¹, J. Jourdan²

¹National Science Center “Kharkov Institute of Physics and Technology”, Kharkov, Ukraine

e-mail: kotlyarv@kipt.kharkov.ua

²Departement für Physik und Astronomie, Universität Basel, Basel, Switzerland

e-mail: juerg.jourdan@unibas.ch

The spin-dependent momentum distributions (SDMDs) of nucleons and proton-deuteron clusters in polarized ³He and ³H nuclei are studied with wave functions (WFs) for realistic models of nuclear forces.

PACS: 21.45.+v, 27.10.+h, 03.65.Ge, 4.70.+s, 25.20.-x

1. INTRODUCTION

Several representation of a 3N bound state WF have been proposed to incorporate specific features, e.g. symmetry properties, inherent to the system. The WF depending on Jacobi coordinates ρ, r or on relative momenta p, q is expressed [1] in terms of functions and spin-isospin states that belong to irreducible representations of symmetric group S_3 . Within approach [2] the WF is written as an operator acting on a 3N spin state. The operator is constructed from the Jacobi vectors and spin matrices with coefficients that are scalar functions of the magnitudes $|\rho|, |r|$ and the angle between them.

Recently, the representation of eight scalar functions [2] in a form of partial wave decompositions in the momentum space is obtained [3]. The partial-wave basis is very useful [4,5] for getting numerical solutions of the Faddeev equations and for computing the amplitudes of diverse processes that include 3N systems.

Studies of ³He two-body photodisintegration [6-8] at energies both below and above the pion production threshold have demonstrated that the corresponding amplitudes can be calculated in momentum space not employing partial wave decompositions but with the WF in vector variables. In [6-8] the plane wave approximation is adopted and two-nucleon interaction currents are included.

In this paper we cast WF [6-8] into a simple functional form that involves scalar functions of $|\rho|, |q|$ and $p \cdot q$. Representations for the WF that are analogous to one proposed in [2] are derived and then employed in analysis of the SDMDs. Some common peculiarities in manifestation of the WF components with non-zero angular orbital momenta in the SDMDs and the cross section for γ ³He \rightarrow pd are considered.

2. WAVE FUNCTION OF 3N BOUND STATE

Three-nucleon bound state $|\Psi_{m'}\rangle = |\Psi, 1/2, m'\rangle$ with total angular momentum $I = 1/2$ and its projection on the z -axis m' can be conveniently represented as a superposition of spin states

$$|\Psi_{m'}\rangle = \sum_{SMm} \Psi_{m'}^{SMm} |SM\rangle_{23} |1/2 m\rangle_1. \quad (1)$$

The eigenstates of the spin operator of the i th nucleon squared $s^2(i)$ and $s_z(i)$ are $|1/2 m_i\rangle_i$, where spin projection of the nucleon is m_i , $i = 1, 2, 3$. The eigenvectors of S^2 and S_z are $|SM\rangle_{23}$, where $S = s(2) + s(3)$.

The ³He WFs used in [6-8] and in this paper

$$\Psi_{m'}^{SMm}(p, q, T) = \langle p, q | \langle SM, 1/2 m | \langle (T 1/2) \square = 1/2, M_\square | \Psi_{m'} \rangle. \quad (2)$$

correspond to projections of the coefficients $\Psi_{m'}^{SMm} = {}_{23,1} \langle SM, 1/2 m | \Psi_{m'} \rangle$ on the eigenvectors of relative momenta, and the isospin states $|(T 1/2) \square M_\square\rangle_{23,1}$, where $T=0,1$ stands for the isospin of nucleons 2 and 3, $\square = 1/2, 3/2$ and M_\square are the total isospin of the nucleus and its projection.

The sum over spin S in Eq. (1) can be transformed in such a way as to eliminate state $|1M\rangle_{23}$

$$|\Psi_{m'}\rangle = \sum_m (\Psi_{m'}^{00m} + \sum_M \Psi_{m'}^{1Mm} \sigma_M(23)) |00\rangle_{23} |1/2 m\rangle_1. \quad (3)$$

The identity $|1M\rangle_{23} = \sigma_M(23) |00\rangle_{23}$, where $\sigma(23) = 1/2 (\sigma(2) - \sigma(3))$, is used with this end. The Pauli vector in the spin space on nucleon i is $\sigma(i)$. For the covariant and contravariant cyclic components of vectors and tensors we refer at [9].

With the aim to reduce the sum over m in Eq. (1) we note $\Psi_{m'}^{SMm} = {}_{23} \langle SM | \Psi_{m'}^m \rangle$ and decompose vector $|\Psi_{m'}^m\rangle = {}_1 \langle 1/2 m | \Psi_{m'} \rangle$ in the spin space of nucleons 2,3 as

$$|\Psi_{m'}^m\rangle = \delta_{mm'} |\Psi_{00}\rangle + \sum_M \langle m | \sigma^M | m' \rangle |\Psi_{1M}\rangle. \quad (4)$$

The shorthand notation $\langle m | \sigma | m' \rangle = \langle 1/2 m | \sigma | 1/2 m' \rangle$ is employed in Eq. (4) and below.

Taking advantage of Eqs. (3) and (4) we write the vector of three-nucleon bound state (1) as

$$|\Psi_{m'}\rangle = \hat{\Psi} |00\rangle_{23} |1/2 m'\rangle_1, \quad (5)$$

where operator $\hat{\Psi} = \sum_{\lambda=1,\dots,4} \hat{\Psi}_\lambda$ can be projected, like $\Psi_{m'}^{SMm}$, on the vectors $|\rho, r\rangle$ or $|p, q\rangle$ as well as on an isospin basis.

Expansion of $|\Psi_{m'}\rangle$ over the 3N states with defined values of the total spin Σ is commonly used. The operator $\hat{\Psi}$ applied to $|S=M=0\rangle_{23}|1/2 m'\rangle_1 = |(S=0, 1/2)\Sigma=1/2, M_\Sigma\rangle$ generates vectors with $S=0$, $\Sigma=1/2$ and $S=1$, $\Sigma=1/2, 3/2$.

Terms $\hat{\Psi}_1 = \Psi_{00}^{00}$ and $\hat{\Psi}_2 = \sum_M \Psi_{1M}^{00} \sigma^M$ (1) produce components of $|\Psi_{m'}\rangle$ with $S=0$ and $\Sigma=1/2$. The spin states created by $\hat{\Psi}_{\lambda=1}$ have $M_\Sigma = m'$. The projections M_Σ and m' may differ from each other for the components originating from $\hat{\Psi}_\lambda$ with $\lambda=2, 3, 4$.

Spin states with $S=1$ and $\Sigma=1/2$ or $3/2$ spring from $\hat{\Psi}_\lambda$ with $\lambda=3, 4$. Similarly to $\hat{\Psi}_{\lambda=2}$, operator $\hat{\Psi}_{\lambda=3}$ is a convolution $\hat{\Psi}_3 = \sum_M \Psi_{00}^{1M} \sigma^M$ (23) of the Pauli matrices and the quantity Ψ_{00}^{1M} that transforms under space rotations like a vector

Expansion of $\hat{\Psi}_{\lambda=4}$ includes spin matrices for nucleon with number 1 and for subsystem 2,3

$$\hat{\Psi}_4 = \sum_{MM'} \Psi_{1M}^{1M'} \sigma^{M'} (1) \sigma^M (23) \quad (6)$$

coupled by a rank two tensor $\Psi_{KM'}^{SM} = {}_{23}\langle SM | \Psi_{KM'} \rangle$.

Since our calculations are performed with ${}^3\text{He}$ WF in the momentum representation, we consider the function $|\Psi_{m'}(p, q)\rangle = \langle p, q | \Psi_{m'} \rangle$ that depends on the reducible tensor $\Psi_{KM'}^{SM}(p, q) = \langle p, q | {}_{23}\langle SM | \Psi_{KM'} \rangle$. The tensor is to be constructed from the momenta p, q and scalar functions $\psi_\nu = \psi(|p|, |q|, \xi; \nu)$, where $\xi = \hat{p} \cdot \hat{q}$, \hat{n} is a unit vector in the n -direction, ν labels the functions.

We project Eq. (5) on vectors $\langle p, q |$ and express the operators $\hat{\Psi}_\nu(p, q)$ in terms of the scalar functions employing the Cartesian basis. It is assumed that the 3N bound state has positive parity.

First term in $\hat{\Psi}$ is the unit operator $\hat{\Psi}_1(p, q) = \psi_1$. For brevity we denote $\sigma_i = \sigma(i)$ and $\sigma_{23} = \sigma(23)$. Next two contributions include one spin operator

$$\hat{\Psi}_2(p, q) = \Psi_2(p, q) \cdot \sigma_1, \quad \hat{\Psi}_3(p, q) = \Psi_3(p, q) \cdot \sigma_{23}$$

Pseudovectors $\Psi_\lambda(p, q)$ can be written as

$$\Psi_\lambda(p, q) = i[\hat{p} \times \hat{q}] \psi_\lambda, \quad (\lambda = 2, 3).$$

Eq. (6) yields $\hat{\Psi}_4(p, q) = \sum_{nn'} \Psi_{nn'}(p, q) \sigma_n(1) \sigma_{n'}(2, 3)$.

The function $\Psi_{nn'}(p, q)$, where $n, n' = x, y, z$, is equivalent to tensor $\Psi_{1M}^{1M'}(p, q)$. It includes a part that is proportional to the unit matrix, as well as antisymmetric and symmetric irreducible tensors

$$\Psi_{nn'}(p, q) = \delta_{nn'} \psi_4 + \Psi_{nn'}^{antisym} + \Psi_{nn'}^{sym}. \quad (7)$$

The antisymmetric term on the r.h.s. of Eq. (7) reads

$$\Psi_{nn'}^{antisym}(p, q) = \sum_{klr} \epsilon_{nn'k} \epsilon_{klr} \hat{p}_l \hat{q}_r \psi_5.$$

Another three functions ψ_ν are to be introduced with the aim to parametrize the symmetric tensor in (7)

$$\Psi_{nn'}^{sym}(p, q) = \hat{p}_n \hat{p}_{n'} \psi_6 + \hat{q}_n \hat{q}_{n'} \psi_7 + (\hat{p}_n \hat{q}_{n'} + \hat{q}_n \hat{p}_{n'}) \psi_8.$$

Thus, we arrive at representation of a 3N bound state in the form of the spin operator $\hat{\Psi}(p, q)$ applied to the spin state with $S=0$ for the pair of nucleons

$$|\Psi_{m'}(p, q)\rangle = \hat{\Psi}(p, q) |(0, 1/2) 1/2, m'\rangle. \quad (8)$$

Eight independent functions $\psi(p, q, \xi; \nu)$ are to be determined in order to build operator $\hat{\Psi}(p, q)$. Proper transformation properties of the WF with respect to time reversal $\hat{\Pi}$ are provided when all $\psi(p, q, \xi; \nu)$ are real functions.

From the above expressions for $\hat{\Psi}_\lambda(p, q)$ we obtain $\hat{\Psi}(p, q) = \psi_1 + i[\hat{p} \times \hat{q}] \cdot (\psi_2 \sigma_1 + \psi_3 \sigma_{23}) + \psi_4 \sigma_1 \cdot \sigma_{23} + \sigma_1 \cdot \hat{p} \sigma_{23} \cdot \hat{q} (\psi_5 + \psi_8) + \sigma_1 \cdot \hat{q} \sigma_{23} \cdot (\hat{q} \psi_6 + \hat{p}(-\psi_5 + \psi_8))$ (9)

The components of the WF

$$\Psi_{m'}^{SMm}(p, q) = \langle p, q | {}_{23,1}\langle SM, 1/2 m | \Psi_{m'} \rangle \quad (10)$$

with $S=0$ depend upon two scalar functions

$$\Psi_{m'}^{00m}(p, q) = \delta_{mm'} \psi_1 + i[\hat{p} \times \hat{q}] \cdot \langle m | \sigma | m' \rangle \psi_2, \quad (11)$$

The part of WF (10) with $S=1$ involves the other six functions $\psi(p, q, \xi; \nu)$ with $\nu = 3 \dots 8$

$$\begin{aligned} \Psi_{m'}^{1Mm}(p, q) = & \delta_{mm'} i[\hat{p} \times \hat{q}]^M \psi_3 + \sum_{M'} \langle m | \sigma^{M'} | m' \rangle \times \\ & \times (\delta_{MM'} \psi_4 + (p_{M'} q^M - q_{M'} p^M) \psi_5 + \\ & + p_{M'} p^M \psi_6 + q_{M'} q^M \psi_7 + (p_{M'} q^M + q_{M'} p^M) \psi_8). \end{aligned} \quad (12)$$

Eight complex components of WF (10) with $SM=00, 11, 10, 1-1$ and $m, m' = \pm 1/2$ are expressed via Eqs. (11) and (12) in terms of real scalar functions $\psi(p, q, \xi; \nu)$, where $\nu = 1 \dots 8$. Space inversion $\hat{\Pi}$ and time reversal $\hat{\Pi}$ results [6] in $\Psi_{m'}^{SMm}(p, q) = (-1)^{S+M+m-m'} (\Psi_{-m'}^{S, -M, -m}(p, q))^*$ i.e., four complex components of WF (10) are independent.

3. SPIN-DEPENDENT MOMENTUM DISTRIBUTIONS OF NEUTRONS AND PROTONS

The density matrix [10,11] of a free nucleon that is in the spin state coinciding with its spin state inside a nucleus is $\langle 1/2 \tilde{m} | \rho(\mu, m') | 1/2 m \rangle = \delta_{\tilde{m}m} w(m, \mu, m')$, where $\mu = \pm 1/2$ is the projection of nucleon isospin and $w(m, \mu, m') = R(m, \mu, m') / \sum_{m''} R(m'', \mu, m')$. The nuclear matrix elements $R(m, \mu, m') = \langle \Psi_{m'} | P_m(1) P_\mu(1) | \Psi_{m'} \rangle$ involve the spin and isospin projection operators $P_m(i) = 1/2(1 + 2m\sigma_z(i))$, and $P_\mu(i) = 1/2(1 + 2\mu\tau_z(i))$, where i is the nucleon number. Nucleon polarization is an integral quantity that is given by

$$P(\mu) = w(m = 1/2, \mu, m') - w(m = -1/2, \mu, m').$$

In this paper we perform calculations with the WFs for Reid soft core (RSC), Paris, Bonn, Argonne AV18 nucleon-nucleon potentials and AV18 in junction with the Urbana IX model of 3N forces (UrbIX). The WFs are constructed from the partial wave components $\Psi_\alpha^{(1)}(p, q)$ with $\alpha = 1 \dots 5$ from Ref. [12] in the case of the RSC potential and $\Psi_\alpha(p, q)$ with $\alpha = 1 \dots 34$

from [4,13] for modern models of nuclear forces. The sets of quantum numbers in (jJ)-coupling are marked by α .

As seen from the table, the neutron polarization $P(\mu = -1/2) \approx 90\%$ that agrees with [10,11,14]. The proton polarization is negative and small. The values of $P(\mu = \pm 1/2)$ appear to be only weakly dependent on model of nuclear forces.

Polarization of nucleons in ${}^3\text{He}$ nucleus

Model of nuclear forces	$P(\mu=-1/2)$	$P(\mu=+1/2)$
AV18UrbIX	0.87	-0.026
AV18	0.88	-0.023
Bonn	0.90	-0.020
Paris	0.88	-0.023
RSC	0.87	-0.025

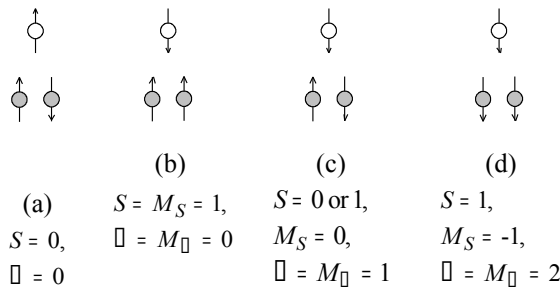


Fig. 1. Spin states, spin S of proton pair and values of \square for some components of the 3N WF with $I = m' = 1/2$. Neutrons (open circles) are in the states with $m_n = +1/2$ ($-1/2$) for the configurations shown in the panel (a) ((b), (c), (d)). Protons are indicated by the filled circles

For the 3N states shown in panel (a) of Fig. 1 we have $P(\mu = -1/2) = 1$. For these components of the WF the spin of the nucleus is carried by the neutron alone and the projection of total \square angular momentum for the 3N system $m' = M_\square + M_S + m_n$ is $m' = m_n$. Samples of the WF components with $m_n = -1/2$ and total orbital momentum $\square = 0, 1, 2$ that reduce the neutron polarization are displayed in panels (b), (c) and (c) in the figure.

More detailed information on the spin structure of 3N bound state can be obtained from SDMDs

$$n(q, m, \mu = 1/2, m') = n(q, m, T = 0, m') + 1/3 n(q, m, T = 1, m'),$$

$$n(q, m, \mu = -1/2, m') = 2/3 n(q, m, T = 1, m'),$$

where $n(q, m, T, m') = 4\pi \sum_{SM} |\Psi_m^{SM}(p, q; T)|^2 d^3 p$ are the SDMDs with defined values of isospin T . Components of the 3N WF with $\square = 3/2$ are not discussed in the present paper. The SDMDs for proton (neutron) in ${}^3\text{He}$ do not differ visibly from ones for neutron (proton) in ${}^3\text{H}$.

Calculations with the WFs for RSC, Paris, Bonn, AV18 and AV18UrbIX demonstrate that the neutron momentum distribution MD $n(q, \mu = -1/2)$ is sensitive to internucleon potential at $q \approx 300$ MeV/c, where $n(q, \mu) =$

$= 1/2 \sum_{m, m'} n(q, m, \mu, m')$. One can expect that in this region the WFs and MDs are influenced not only by one-pion tail of the nuclear forces, but are sensitive to short-range behavior of the nuclear forces and the WF.

$$\alpha(q, \mu) = (n(q, m = 1/2, \mu, m') - n(q, m = -1/2, \mu, m')) / n(q, \mu) |_{m' = 1/2}, \quad (13)$$

obtained with WF [13] for AV18UrbIX interaction, are shown in Figs. 3...5 for $q = (q_x, q_y = 0, q_z)$.

The MD can be written as the sum of SDMDs $n(q) = 1/2 \sum_{m, \mu, m'} n(q, m, \mu, m')$. Calculations of MD are compared in Fig. 2 with the results of y-scaling analysis [15] for inclusive reaction ${}^3\text{He}(e, e')X$ and with data [16, 17] obtained from exclusive experiments ${}^3\text{He}(e, e'p)d$ and ${}^3\text{He}(e, e'p)np$ within approximate treatment of exchange currents and rescattering effects.

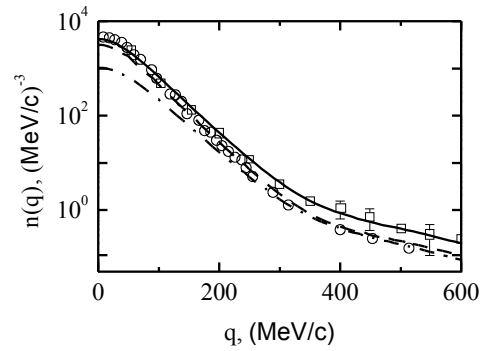


Fig. 2. Momentum distribution $n(q, \mu)$ of nucleons in ${}^3\text{He}$ nucleus. Dashed (dot-dashed) curve represents the proton (neutron) distribution. Solid curve is their sum $n(q)$. The calculations are performed with the WF for AV18UrbIX model of nuclear forces

Since $\alpha(q, \mu)$ are invariant under the transformations $q = (q_x, q_y, q_z) \rightarrow (\varepsilon_x q_x, \varepsilon_y q_y, \varepsilon_z q_z)$, where $\varepsilon_n = \pm 1$, ($n = x, y, z$), as well as under an arbitrary rotation about the z -axis, the level lines displayed in Figs. 3 and 4 allow one to restore space distributions for the asymmetries.

Comparing Figs. 3 and 4 we see that the dependence of the asymmetry $\alpha(q, \mu)$ for proton on components of vector q is in sharp contrast to one for neutron. At low values of $|q|$, oriented ${}^3\text{He}$ nuclei can serve as an effective polarized neutron target (EPNT). This area of momentum transfer could be achieved in experiments at an electron accelerator discussed in Ref. [19]. According to Fig. 3, polarized ${}^3\text{H}$ nuclei may be used for devising an EPNT for experiments where $|q_x| \approx 200$ MeV/c and $450 < |q_z| \leq 800$ MeV/c or $400 \leq |q_z| \leq 650$ MeV/c and $|q_z| \leq 200$ MeV/c.

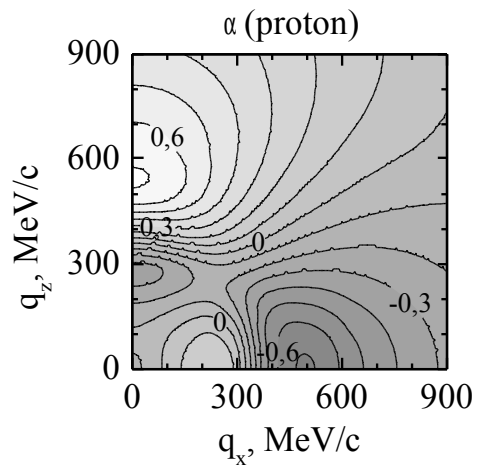
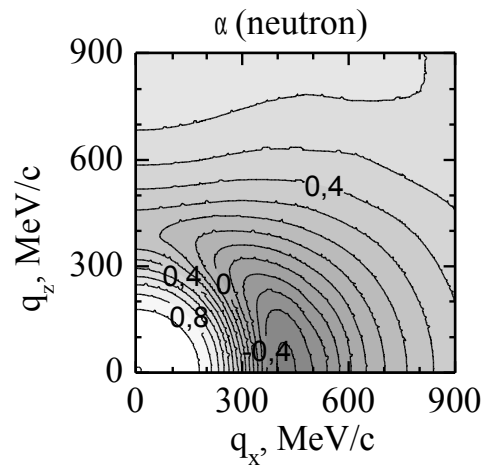


Fig. 3. Asymmetry of SDMDs of proton

Fig. 4. Asymmetry of SDMDs of neutron



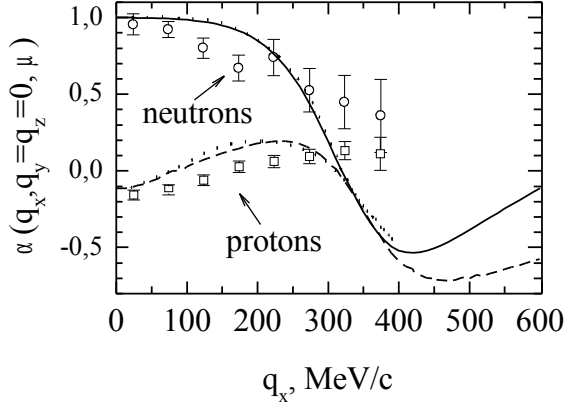


Fig. 5. Asymmetry of SDMDs of neutron and proton (solid and dashed curves). Results of calculations [18] are displayed by dotted curve. Data shown by circles are obtained in [18] from PWIA analysis of measured spin asymmetries in ${}^3\text{He}(p,2p)$ and ${}^3\text{He}(p,pn)$

Figs. 5 shows that the asymmetries as functions of q_x at $q_y = q_z = 0$ calculated in the present paper (solid and dashed curves) and in [18] (dotted curves) are in quite good agreement. The apparent discrepancy between theory and experiment at $q_x \gtrsim 300\text{MeV}/c$ may stem, e.g., from the neglect of corrections due to antisymmetrization of final states and rescattering effects in the PWIA treatment [18] of the measured spin asymmetries.

To analyze properties of the SDMDs we consider

$$n_{\vec{m}\vec{m}'}^{\vec{m}\vec{m}'}(q, T) = 4\pi \sum_{SM} |(\Psi_{\vec{m}\vec{m}'}^{SM\vec{m}}(p, q; T))^* \Psi_{\vec{m}\vec{m}'}^{SMm}(p, q; T)|^2 d^3p. \quad (14)$$

The SDMD is the diagonal part of tensor (14)

$$n(q, m, T, m') = n_{\vec{m}\vec{m}'}^{\vec{m}\vec{m}'}(q; T) |_{\vec{m}'=m', \vec{m}=m}$$

With the 3N bound-state vector in form (4) we get

$$n_{\vec{m}\vec{m}'}^{\vec{m}\vec{m}'}(q; T) = 1/2 (\delta_{\vec{m}\vec{m}'} \delta_{mm'} \tilde{h}_0 + \langle \vec{m}' | \sigma | \vec{m} \rangle \langle m | \sigma | m' \rangle \tilde{h}_1 + \langle \vec{m}' | \sigma \cdot \hat{q} | \vec{m} \rangle \langle m | \sigma \cdot \hat{q} | m' \rangle \tilde{h}_2), \quad (15)$$

where structure functions (SFs) $\tilde{h}_i = \tilde{h}_i(q, T)$, ($i=0,1,2$).

The MD $n(q, T) = 1/2 \sum_{m, m'} n(q, m, T, m')$ is given by $n(q, T) = 1/2 (\tilde{h}_0 + 3\tilde{h}_1 + \tilde{h}_2)$. The asymmetry of SDMDs is

$$\alpha(q, \mu) n(q, \mu) |_{\mu = -1/2} = 1/2 (\tilde{h}_0 - \tilde{h}_1 + (2q_z^2/q^2 - 1)\tilde{h}_2).$$

Alternatively, one can use the space rotations, the \hat{P} - and \hat{Q} - transformation to ascertain in analogy with non-central NN interaction [20] that

$$n_{\vec{m}\vec{m}'}^{\vec{m}\vec{m}'}(q, T) = 1/2 (\delta_{\vec{m}\vec{m}'} \delta_{mm'} h_0 + \langle m | \sigma | \vec{m} \rangle \langle \vec{m}' | \sigma | m' \rangle h_1 + \langle m | \sigma \cdot \hat{q} | \vec{m} \rangle \langle \vec{m}' | \sigma \cdot \hat{q} | m' \rangle h_2), \quad (16)$$

with SFs $h_i = h_i(q, T)$, ($i = 0, 1, 2$). Eq. (16) agrees in form with the representation for the spectral function discussed in [11] and is convenient for analyzing q -dependence of the SDMDs and of the corresponding asymmetry. In terms of the SFs h_i we have for the MD $n(q, T) = h_0$ and for the asymmetry

$$\alpha(q, \mu = -1/2) n(q, \mu = -1/2) = h_1 + q_z^2/q^2 h_2.$$

Recoupling spins in (15) we find the relations between the different sets of SFs $h_0 = 1/2 (\tilde{h}_0 + 3\tilde{h}_1 + \tilde{h}_2)$, $h_1 = 1/2 (\tilde{h}_0 - \tilde{h}_1 - \tilde{h}_2)$ and $h_2 = \tilde{h}_2$.

4. SPIN-DEPENDENT MOMENTUM DISTRIBUTIONS OF PROTON-DEUTERON CLUSTERS

MD of pd-clusters in ${}^3\text{He}$ $\rho(q) = 1/2 \sum_{Mmm'} \rho_{Mmm'}(q)$ is the sum of SDMDs $\rho_{Mmm'}(q) = 3 |A_m^{Mm}(q)|^2$, where $A_m^{Mm}(q) = \sum_{M'} |(\varphi_{M'}^M(p))^* \Psi_m^{1M'm}(p, q; 0)|^2 d^3p$. The deuteron WF is $\varphi_{M'}^M(p) = \langle p, S=1, M, T=M_T=0 | \varphi, I=1, M' \rangle$. The overlap integrals receive contributions only from partial-wave components of the ${}^3\text{He}$ WF with quantum numbers $2S+1L_J l_j = {}^3S_1 S_{1/2}, {}^3D_1 S_{1/2}, {}^3S_1 D_{3/2}, {}^3D_1 D_{3/2}$. As is known (see, e.g., [21]), computation of quantities $A_m^{Mm}(q)$ with functions $\Psi_\alpha(p, q)$ is straightforward.

In the present paper we are following [22] and calculate $A_m^{Mm}(q)$ with WF in representation (2) employing the vector variables. While results of report [22] were obtained with parametrization [12] of $\Psi_\alpha^{(1)}(p, q)$ for the RSC potential, here we use the components [4,13] of $\Psi_\alpha(p, q)$ for contemporary model of nuclear forces.

Figs. 6 and 7 show normalized SDMDs $r_{M_d m m'}(q) = \rho_{M_d m m'}(q) / \rho(q)$ for $q = (q_x, q_y=0, q_z)$. As seen from Fig. 6, the SDMD with $M_d=1$ (i.e., when spins of the neutron the nucleus are parallel) has no maximum at small values of $|q|$, that is at variance with behavior of the neutron asymmetry in Fig. 4. This observation may serve as an indication that pd-clusters do not dominate in structure of ${}^3\text{He}$ in this area of q .

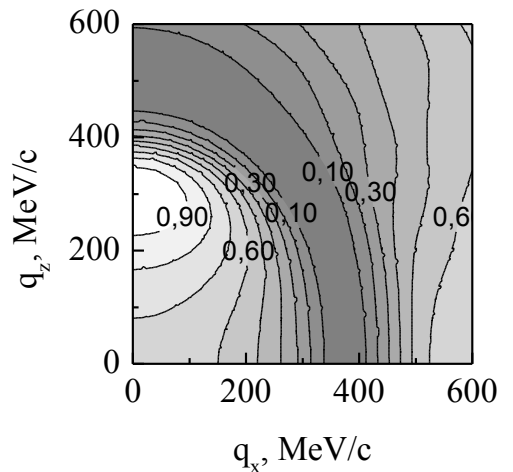


Fig. 6. MD $r_{M_d m m'}(q)$ with $M_d, m, m' = 1, -1/2, 1/2$

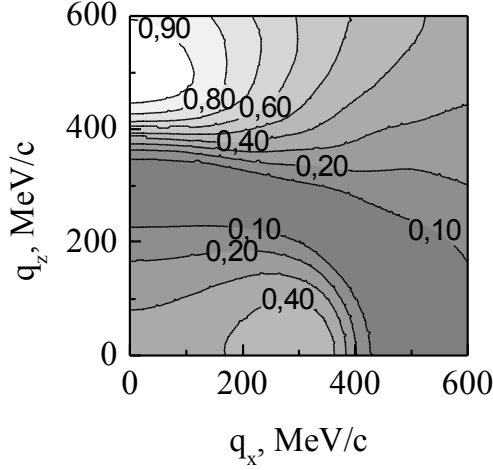


Fig. 7. $MD r_{M_d m m'}(q)$ with $M_d, m, m' = 0, 1/2, 1/2$

The SDMD in Fig. 7 characterizes probability to find a proton-deuteron cluster in ${}^3\text{He}$ with parallel spins of the proton, being nucleon with number 1, and the nucleus. Observed maximum in the SDMD at $q_x \approx 100$ MeV/c and $q_z > 500$ MeV/c conforms with one appropriate to the proton asymmetry in the same q -region (see Fig. 3).

5. DISCUSSION

Spin asymmetries for disintegration of polarized ${}^3\text{He}$ target are intensively studied at Mainz [23,24] and JLab [25] in experiments with longitudinally polarized electron beams. Within the PWIA, the polarization observables for the processes with polarized target and with polarized beam or outgoing particles are directly related to asymmetries of SDMDs considered in sect. 2 and 3.

The SDMDs prove to be strongly dependent on the components of the ${}^3\text{He}$ WF with non-zero values of orbital angular momenta L, l . Nevertheless, usage of the data to disentangle contributions of these components is, in general, complicated (see, e.g., [5,6]) by the reaction mechanisms that are not included in PWIA, in particular by rescattering in the final state or interaction currents. It was found that the relative role of the mechanisms strongly varies with the kinematics of the processes.

We face a similar situation [8] in the case of the differential cross section $\sigma = \sigma(E_\gamma, \theta_p)$ for $\gamma {}^3\text{He} \rightarrow \text{pd}$. Energy dependence of σ , computed with the convection (CC) and spin currents (SC), changes quantitatively (see Fig. 8.) by components of the WF with $L, l > 0$. S-waves with $L=l=0$ are labeled by $\alpha = 1, 2$. States with $\alpha = 3, 4, 5$ contain the D-waves with $L=l= 20, 02$ and 22 . The P-waves with $J=0, 1$ correspond to $\alpha = 6 \dots 10$. The set of the partial-waves with $\alpha \leq 18$ (34) involves components with $J \leq 2$ (4). The appreciable sensitivity of σ ultimately disappears when meson exchange currents of pion range (πEC) are added to CC and SC. The spin-orbit (SOC) current does not modify visibly $\sigma(E_\gamma, \theta_p = 90^\circ)$.

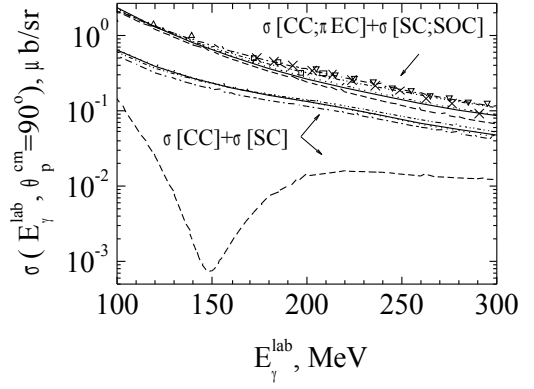


Fig. 8. Dependence of the differential cross section for $\gamma {}^3\text{He} \rightarrow \text{pd}$ on the components of the ${}^3\text{He}$ WF. Calculations with the WF for the AV18UrbIX interaction are presented. Dashed, dash-dotted, dash-dot-dotted, dotted and solid curves are obtained with $\alpha = 2, 5, 10, 18, 34$, respectively. The data $\square, \square, \square, \times$ are from [26-29]

Influence of the partial-wave components of the WF and the πEC on the observables for $\gamma {}^3\text{He} \rightarrow \text{pd}$ and $e {}^3\text{He} \rightarrow e' \text{pd}$ was discussed in [6-8] and [22]. The representations for the 3N bound-state WF derived in the present paper are of interest for interpretation of qualitative features in behavior of energy and angular distributions of the observables.

The author (VK) is grateful to A. Nogga, H. Kamada, W. Glöckle, J. Gólak and H. Witała for partial-wave components of the ${}^3\text{He}$ WF.

REFERENCES

1. A.G. Sitenko, V.F. Kharchenko. Bound states and scattering in system of three particles // *Uspehi Fiz. Nauk.* 1971, v. 103, p. 467-525 (in Russian).
2. E. Gerjuoy, J. Schwinger. On Tensor Forces and the Theory of Light Nuclei // *Phys. Rev.* 1942, v. 61, p. 138-146.
3. I. Fachruddin, W. Glöckle Ch. Elster A. Nogga. Operator form of ^3H (^3He) and its spin structure // *Phys. Rev. C.* 2004, v. 69, 064002, 16 p.
4. W. Glöckle, H. Witała, D. Hüber et al. The Three-Nucleon Continuum: Achievements, Challenges and Applications // *Phys. Rep.* 1996, v. 274, p. 107-286.
5. J. Golak, R. Skibiński, H. Witała et al. *Electron and Photon Scattering on Three-Nucleon Bound States.* nucl-th/0505072, 2005, 154 p.
6. V. Kotlyar, Yu.P. Mel'nik, A.V. Shebeko. Polarization phenomena in photo-and electrodisintegration of the lightest nuclei at medium energies // *Phys. Part. and Nucl.* 1995, v. 26, №1, p. 79-113.
7. A.A. Belyaev, J. Golak, W. Glöckle et al. Off-Shell Effects in Electromagnetic Interaction with Bound Nucleons // *Problems of Atomic Science and Technology. Series: Nuclear Physics Investigations.* 2001, №6(1), p. 187-191.
8. V. Kotlyar, A. Nogga, H. Kamada et al. *Mechanisms of two-body ^3He photodisintegration above the pion production threshold* Proc. 17th Int. IUPAP Conf. on Few-Body Problems in Phys. Durham, North Carolina, USA, 2003. Eds. W.Glöckle et al. p. 210-211.
9. D.A. Varshalovich, A.N. Moskalev, V.K. Khersonskii, *Quantum Theory of Angular Momentum,* World Scientific, Singapore, 1989, 439 p.
10. J.L. Friar, B.F. Gibson, G.L. Payne et al. Neutron polarization in polarized ^3He targets // *Phys. Rev. C.* 1990, v. 42, p. 2310-2314.
11. R.-W. Schulze, P.U. Sauer. Inelastic electron scattering from the three-nucleon bound states with polarization // *Phys. Rev. C.* 1993, v. 48, p. 38-63.
12. Ch. Hajduk, A.M. Green, M.E. Sainio. A convenient analytical form for the triton wave function // *Nucl. Phys. A.* 1980, v. 337, p. 13-22.
13. A. Nogga, H. Kamada, W. Glöckle, B.R. Barrett. The α particle based on modern nuclear forces // *Phys. Rev. C.* 2002, v. 65, 054003, 18 p.
14. B. Blankleider, R.M. Woloshyn. Quasielastic scattering of polarized electrons on polarized ^3He // *Phys. Rev. C.* 1984, v. 29, p. 538-552.
15. C. Ciofi degli Atti, S. Simula. Realistic model of the nucleon spectral function in few and many nucleon systems // *Phys. Rev. C.* 1996, v. 53, p. 1689-1710.
16. E. Jans, M. Bernheim, M.K. Brusseet et al. The quasi-free $^3\text{He}(e,e'p)$ reaction // *Nucl. Phys. A.* 1987, v. 475, p. 687-719.
17. C. Marchand, M. Bernheim, P.C. Dunn et al. High proton momenta and nucleon-nucleon correlations in the reaction $^3\text{He}(e,e'p)$ // *Phys. Rev. Lett.* 1988, v. 60, p. 1703-1706.
18. R.G. Milner, C. Bloch, J.F.J. van den Brand et al. The spin dependent momentum distributions of neutron and proton in ^3He // *Phys. Let. B.* 1996, v. 379, p. 67-72.
19. Yu.M. Arkatov, A.V. Glamazdin, A.N. Dovbnya, I.S. Guk, S.G. Kononenko, F.A. Peev, M. van der Wiel, J.I.M. Botman, A.S. Tarasenko. *Baseline accelerator facility at NSC KIPT for nuclear and high energy physics research, "SALO" Project.* Kharkov, 2004, 94p.
20. L. Eisenbud, E.P. Wigner. *Nuclear structure.* Princeton NJ: "Princeton Univ. Press", 1958, 130 p.
21. J. Golak, W. Glöckle, H. Kamada et al. Spin dependent momentum distributions of proton-deuteron clusters in ^3He from electron scattering on polarized ^3He : theoretical predictions // *Phys.Rev. C.* 2002, v. 65, 064004, 7 p.
22. V.V. Kotlyar. *Calculation of Polarization Observables in Photo- and Electrodisintegration of ^3He .* Proc. 3rd Int. Symp. "Dubna Deuteron-95" Dubna, 1995. Dubna, 1996, p. 221-226.
23. A1 Collab. at MAMI (Mainz): <http://wwwa1.kph.uni-mainz.de/A1/>.
24. P. Achenbach, D. Baumann, R. Böhmer et al. *Measurement of the asymmetries in $^3\text{He}(e, e'p)d$ and $^3\text{He}(e, e'p)np$.* nucl-ex/0505012, 2005, 8 p.
25. TJNAF Polarized ^3He Target Collab.: <http://hallaweb.jlab.org/physics/experiments/he3/pre-f.html>.
26. N.M. Fallon, L.J. Koester, J.H. Smith. Two-body photodisintegration of ^3He between 40 and 150 MeV // *Phys. Rev. C.* 1972, v. 5, p. 1926-1938.
27. N.R. Kolb, E.B. Cairns, E.D. Hackett et al. $^3\text{He}(\gamma, pd)$ cross sections with tagged photons below the Delta resonance // *Phys. Rev. C.* 1994, v. 49, p. 2586-2591.
28. V. Isbert, G. Audit, N. d'Hose et al. Two Body Photodisintegration of ^3He between 200 and 800 MeV // *Nucl. Phys. A.* 1994, v. A578, p. 525-541.
29. P.E. Argan, G. Audit, N.De Botton et al. Two-body photodisintegration of ^3He and ^4He in the $\Delta(1236)$ region // *Nucl. Phys. A.* 1975, v. 237, p. 447-464.

СПИНОВАЯ СТРУКТУРА СВЯЗАННЫХ СОСТОЯНИЙ ТРЕХ НУКЛОНОВ

В. Котляр, J. Jourdan

Волновые функции для реалистических моделей ядерных сил используются для исследования зависящих от спина импульсных распределений нуклонов и нуклон-дейтронных кластеров в поляризованных ядрах ^3He и ^3H .

СПИНОВА СТРУКТУРА ЗВ'ЯЗАНИХ СТАНІВ ТРЬОХ НУКЛОНІВ

В. Котляр, J. Jourdan

Хвильові функції для реалістичних моделей ядерних сил використовуються для дослідження залежних від спина імпульсних розподілів нуклонів і нуклон-дейтронних кластерів у поляризованих ядрах ${}^3\text{He}$ та ${}^3\text{H}$.